Gazeau-Klauder coherent states in one-mode systems with periodic potential

2001 J. Phys. A: Math. Gen. 34 9463

(http://iopscience.iop.org/0305-4470/34/44/308)

INSTITUTE OF PHYSICS PUBLISHING JOURNAL OF PHYSICS A: MATHEMATICAL AND GENERAL

J. Phys. A: Math. Gen. **34** (2001) 9463–9474 PII: S0305-4470(01)25374-8

Gazeau–Klauder coherent states in one-mode systems with periodic potential

J M Hollingworth[1], **A Konstadopoulou**[1], **S Chountasis**[1], **A Vourdas**[1] **and N B Backhouse**[2]

[1] Department of Electrical Engineering and Electronics, University of Liverpool, Liverpool L69 3GJ, UK
[2] Department of Mathematical Sciences, University of Liverpool, Liverpool L69 7ZL, UK

Received 16 May 2001, in final form 21 September 2001
Published 26 October 2001
Online at stacks.iop.org/JPhysA/34/9463

Abstract

Gazeau–Klauder coherent states for a one-mode system with sinusoidal potential, are introduced. Their quantum statistical properties and their uncertainties are studied. The effect of dissipation on these states is estimated. The evolution of the ordinary (Glauber) coherent states in this system, is also studied. It is shown that these states evolve into superpositions of many macroscopically distinguishable states ('multi-Schrödinger cats').

PACS numbers: 42.50.Ar, 03.65.Yz

1. Introduction

Several authors have studied in considerable detail the concept of coherence in various quadratic Hamiltonians in connection with coherent and squeezed states of light. This work has been intimately connected to the experimental production of squeezed light.

The concept of coherence has also been studied in Hamiltonians with various potentials (e.g. [1]) and these studies have been useful in various areas of physics. Coherence is usually related to some symmetry in the system which in some models is apparent and in other models might be hidden. In many cases the various terms of the Hamiltonian are the generators of some Lie algebra. Coherent states for these cases have been studied extensively in the literature (e.g. [2]). There are other more complicated cases where the Hamiltonian is highly nonlinear and where the terms are not generators of a Lie algebra. For such cases a very general study of coherent states has been recently published by Gazeau and Klauder [3, 4].

In section 2 we consider a Hamiltonian with sinusoidal nonlinearity and study its coherence properties. Such Hamiltonians can be used for the description of Josephson devices (e.g. [5]). We note that the displacement operator appears in this Hamiltonian. In section 3 we introduce Gazeau–Klauder (GK) coherent states for our Hamiltonian. We consider a truncated version of these states and show that they evolve into themselves (temporal stability property) with very good accuracy. We also study the uncertainty properties (Δx, Δp) and the quantum statistical

0305-4470/01/449463+12$30.00

properties ($\langle N\rangle$, $g^{(2)}$, etc) of these states. The results provide an example of the theoretical work of [3, 4]. In practical systems, dissipation is an important factor, and its effect on these states is discussed in section 4. In section 5 we consider ordinary coherent states and study how they evolve in these systems in the absence and also in the presence of dissipation. We show in section 6 that in certain cases they evolve into superpositions of many macroscopically distinguishable states ('multi-Schrödinger cats'). The effect of dissipation on these highly sensitive states is quantified. We conclude in section 7 with a discussion of our results.

2. Model

We consider the Hamiltonian

$$H = \omega a^\dagger a - \lambda \cos[\mu a^\dagger + \mu^* a] \tag{1}$$

where $a^\dagger, a$ are creation and annihilation operators correspondingly. In terms of the the displacement operator,

$$D(A) = \exp(A a^\dagger - A^* a) \tag{2}$$

the Hamiltonian can be written as

$$H = \omega a^\dagger a - \frac{\lambda}{2}\left[D(\mathrm{i}\mu) + D(-\mathrm{i}\mu)\right]. \tag{3}$$

We note that the exponential of the displacement operator appears in the time evolution operator $\exp[\mathrm{i}Ht]$, because the displacement operator appears in the Hamiltonian.

The matrix elements of the Hamiltonian with respect to the number eigenstates $|N\rangle$, $|M\rangle$ are

$$H_{MN} \equiv \langle M|H|N\rangle = \omega N \delta(M, N) - \frac{\lambda}{2}\left[\langle M|D(\mathrm{i}\mu)|N\rangle + \langle M|D(-\mathrm{i}\mu)|N\rangle\right] \tag{4}$$

where $\delta(M, N)$ is the Kronecker delta. It is known [6] that

$$\langle M|D(A)|N\rangle = \left[\frac{N!}{M!}\right]^{1/2} A^{M-N} \exp\left(\frac{-|A|^2}{2}\right) L_N^{M-N}(|A|^2) \tag{5}$$

where $L_N^{M-N}(|A|^2)$ are Laguerre polynomials.

Assuming that at time $t = 0$ the system is in a state $|s(0)\rangle$, we have studied numerically the state

$$|s(t)\rangle = \exp[\mathrm{i}Ht]|s(0)\rangle. \tag{6}$$

The infinite-dimensional matrix (H_{MN}) has been truncated to an $(N_{\max}+1)\times(N_{\max}+1)$ matrix. $N_{\max}$ has been taken to be much greater than the average number of photons in the initial state $|s(0)\rangle$:

$$N_{\max} \gg \langle s(0)|a^\dagger a|s(0)\rangle. \tag{7}$$

We then calculated the $\exp(\mathrm{i}Ht)$ and the state $|s(t)\rangle = \exp(\mathrm{i}Ht)|s(0)\rangle$. As a measure of the accuracy of the approximation we calculated the finite sum $\sum_{N=0}^{N_{\max}} |s_N(t)|^2$ as a function of time, where $s_N(t) \equiv \langle N|s(t)\rangle$. In the limit $N_{\max} \to \infty$ it is equal to 1; and in the truncated case it should be very close to 1. In all our results the above sum was greater than 0.99.

We note that in the small $|\mu|$ limit ($|\mu| \ll 1$), the cosine term in the Hamiltonian can be written as

$$\cos(\mu a^\dagger + \mu^* a) \approx 1 - \frac{(\mu a^\dagger + \mu^* a)^2}{2} \tag{8}$$

and the Hamiltonian reduces to the quadratic Hamiltonian

$$H \approx (\omega + \lambda|\mu|^2)a^\dagger a + \lambda\frac{\mu^2}{2}a^{\dagger^2} + \lambda\frac{\mu^{*^2}}{2}a^2 + \lambda\left(\frac{|\mu|^2}{2} - 1\right) \tag{9}$$

which has been studied extensively in conjunction with squeezed states.

In the large $|\mu|$ limit ($|\mu| \to \infty$) it is seen from equation (5) with $A = \mathrm{i}\mu$ that the matrix elements of the cosine term contain the term $\exp(-\frac{|\mu^2|}{2})$. We note that the term $[\frac{N!}{M!}]^{1/2}L_N^{M-N}(|\mathrm{i}\mu|^2)$ increases with μ only in a polynomial way and therefore the matrix elements of the cosine term become practically zero. Therefore in this limit the Hamiltonian is simply a Harmonic oscillator Hamiltonian.

3. Gazeau–Klauder coherent states

Let E_n and $|n;\omega,\lambda,\mu\rangle$ be the eigenvalues and eigenstates of the Hamiltonian (1):

$$H|n;\omega,\lambda,\mu\rangle = E_n|n;\omega,\lambda,\mu\rangle. \tag{10}$$

Following [4], we rescale the eigenvalues:

$$e_n = \frac{E_n - E_0}{\omega} \tag{11}$$

where E_0 is the lowest energy state, and introduce the generalized factorial:

$$\rho_0 = 1 \qquad \rho_n = \rho_{n-1}e_n \qquad n \geqslant 1. \tag{12}$$

The generalized coherent states are introduced as

$$|J,\theta;\omega,\lambda,\mu\rangle = \frac{1}{N(J)}\sum_{n=0}^{\infty}\frac{J^{n/2}\exp(-\mathrm{i}e_n\theta)}{\sqrt{\rho_n}}|n;\omega,\lambda,\mu\rangle \tag{13}$$

where

$$N(J)^2 = \sum_{n=0}^{\infty}\frac{J^n}{\rho_n} \tag{14}$$

and $0 \leqslant J \leqslant R$, where R is the radius of convergence of the series defining $N(J)$. We shall call the states (13) GK coherent states after [4].

We have calculated numerically a truncated version of the GK coherent states. An initial GK coherent state should evolve into another GK coherent state according to the rule [4]

$$\exp(\mathrm{i}Ht)|J,\theta;\omega,\lambda,\mu\rangle = \exp(\mathrm{i}E_0(t))|J,\theta-\omega t;\omega,\lambda,\mu\rangle. \tag{15}$$

In order to quantify this we have calculated the p-distance

$$d_p(\exp(\mathrm{i}Ht)|J,\theta;\omega,\lambda,\mu\rangle, |J,\theta-\omega t;\omega,\lambda,\mu\rangle) \tag{16}$$

where

$$d_p(f,g) = \left(\int |f(x) - g(x)|^p\,\mathrm{d}x\right)^{1/p}. \tag{17}$$

In figure 1 we present the distance (16) with $p = 2$. It is seen that even the truncated GK coherent states which we consider numerically evolve into other states within the 'family' (temporal stability property) with extremely good accuracy, which of course decreases with time. We have also calculated the probability distribution $P(x) = |\langle x|J,\theta;\omega,\lambda,\mu\rangle|^2$. For many values of these parameters it is a Gaussian-like shape, but not always. For example, in figure 2 we present this probability distribution for the GK coherent state

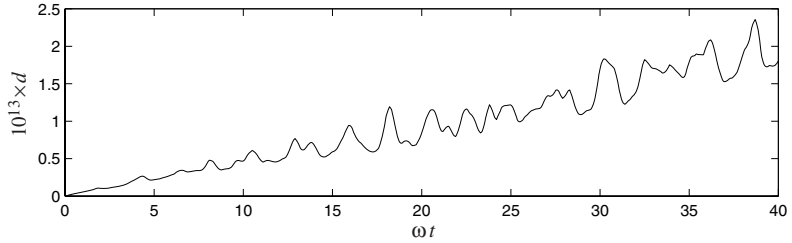

Figure 1. The distance (16) with $p = 2$. We use the Hamiltonian (1) with $\omega = 1$, $\lambda = 1$, $\mu = 1$ and $N_{\max} = 15$. The initial state is the GK coherent state $|J = 2, \theta = 0; \omega, \lambda, \mu\rangle$.

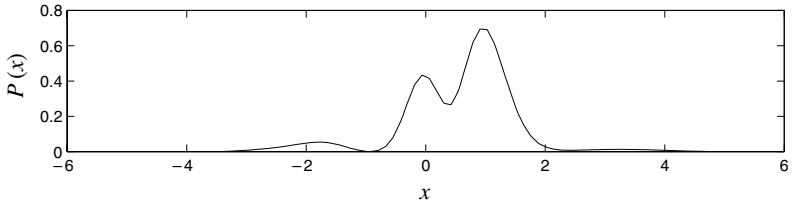

Figure 2. Probability distribution of the GK coherent state $|J = 3, \theta = \pi; \omega = 1, \lambda = 3, \mu = 1\rangle$.

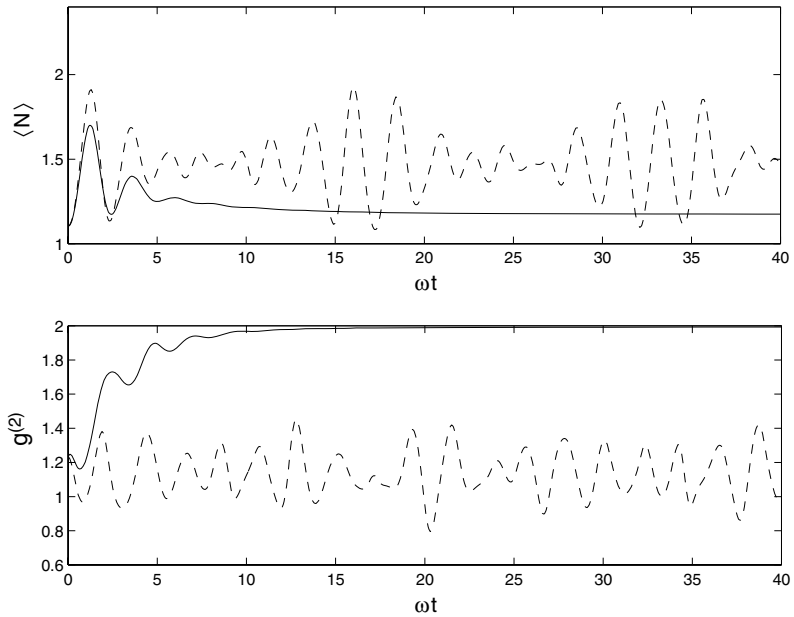

Figure 3. The upper graph shows the average number of photons $\langle N\rangle$ with $\omega = 1$, $\lambda = 1$, $\mu = 1$, $M = 1$, $N_{\max} = 15$ and initial state GK coherent state $|J = 2, \theta = 0; \omega, \lambda, \mu\rangle$. The solid curve shows damped results ($\gamma = 0.2$), and the broken curve shows undamped results ($\gamma = 0$). The lower graph shows the second-order correlation $g^{(2)}$ for the same system (solid curve shows $\gamma = 0.2$, broken curve shows $\gamma = 0$).

$|J = 3, \theta = \pi; \omega = 1, \lambda = 3, \mu = 1\rangle$. It is seen that the probability distribution in this case is different from a Gaussian-like function.

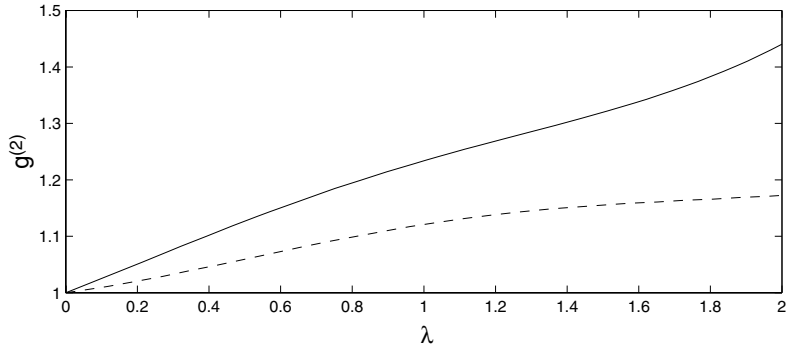

Figure 4. The second-order correlation $g^{(2)}$ for the GK coherent state $|J = 2, \theta = 0; \omega, \lambda, \mu\rangle$ as a function of λ, with $\omega = 1$, $N_{\max} = 15$ and $\mu = 1$ (solid curve), $\mu = 2$ (broken curve).

In figure 3 (broken curve) we present the $\langle N\rangle$

$$\langle N\rangle = \langle s(t)|a^{\dagger}a|s(t)\rangle \tag{18}$$

and the second-order correlation

$$g^{(2)} = \frac{\langle N^2\rangle - \langle N\rangle}{\langle N\rangle^2} = 1 + \frac{Q}{\langle N\rangle} \tag{19}$$

where $Q = \frac{\langle N^2\rangle - \langle N\rangle - \langle N\rangle^2}{\langle N\rangle}$ is the Mandel parameter, as functions of the dimensionless time ωt. It known that for Poissonian distribution $g^{(2)} = 1$ and $Q = 0$. It is seen that both $\langle N\rangle$ and $g^{(2)}$ are oscillatory functions of time.

In figure 4 we present $g^{(2)}$ as a function of λ for $\mu = 1$ (solid curve) and for $\mu = 2$ (broken curve). It is seen that the GK coherent states are not necessarily associated with Poissonian statistics.

In figure 5 we present the uncertainties Δx (curves of crosses), Δp (curves of circles) and the product $\Delta x \Delta p$ (plain curves) as functions of λ, for $\mu = 1$ (solid curve) and $\mu = 2$ (broken curve). It is seen that for $\mu = 1$ the product $\Delta x \Delta p$ becomes slightly greater than 0.5, but that increasing μ to 2 causes the product, and the uncertainties to increase much more rapidly. Therefore the minimum uncertainty property of ordinary coherent states does not hold for GK coherent states.

In figure 6 we present the Wigner function for the GK coherent state $|J = 2, \theta = 0; \omega = 1, \lambda = 1, \mu = 1\rangle$. In this particular example it is seen that the Wigner function is approximately a Gaussian, like an ordinary coherent state.

4. The effect of dissipation on GK coherent states

Dissipation destroys coherence. In order to quantify this we have added damping terms to our model. We solve the following equation:

$$\frac{\partial \rho}{\partial t} = \mathrm{i}[H, \rho] + \frac{\gamma}{2}(M+1)(2a\rho a^{\dagger} - a^{\dagger}a\rho - \rho a^{\dagger}a) + \frac{\gamma}{2}M(2a^{\dagger}\rho a - aa^{\dagger}\rho - \rho aa^{\dagger}) \tag{20}$$

where γ is the damping rate and M is the average number of bath quanta. For a monochromatic bath with frequency ω_B in thermal equilibrium at temperature T,

$$M(\omega_B) = (\mathrm{e}^{\omega_B/T} - 1)^{-1}. \tag{21}$$

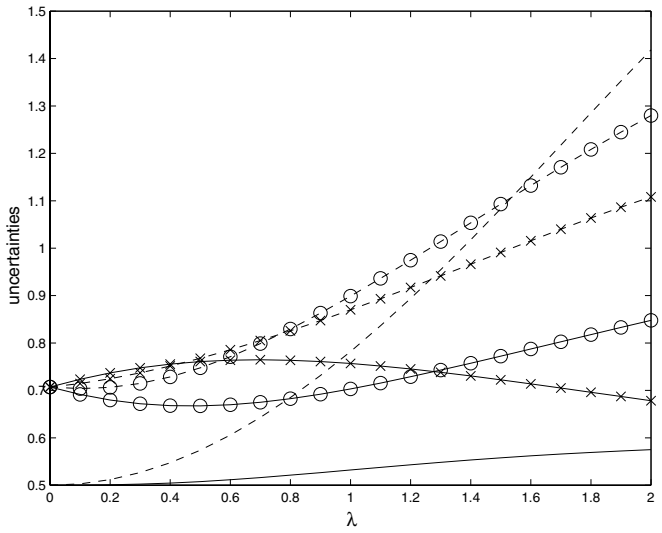

Figure 5. The uncertainties Δx (curves of crosses), Δp (curves of circles) and the product $\Delta x \Delta p$ (plain curves) as functions of λ, for $\mu = 1$ (solid curve) and $\mu = 2$ (broken curve) for the GK coherent state $|J = 2, \theta = 0; \omega, \lambda, \mu\rangle$, with $\omega = 1$, $N_{\max} = 15$.

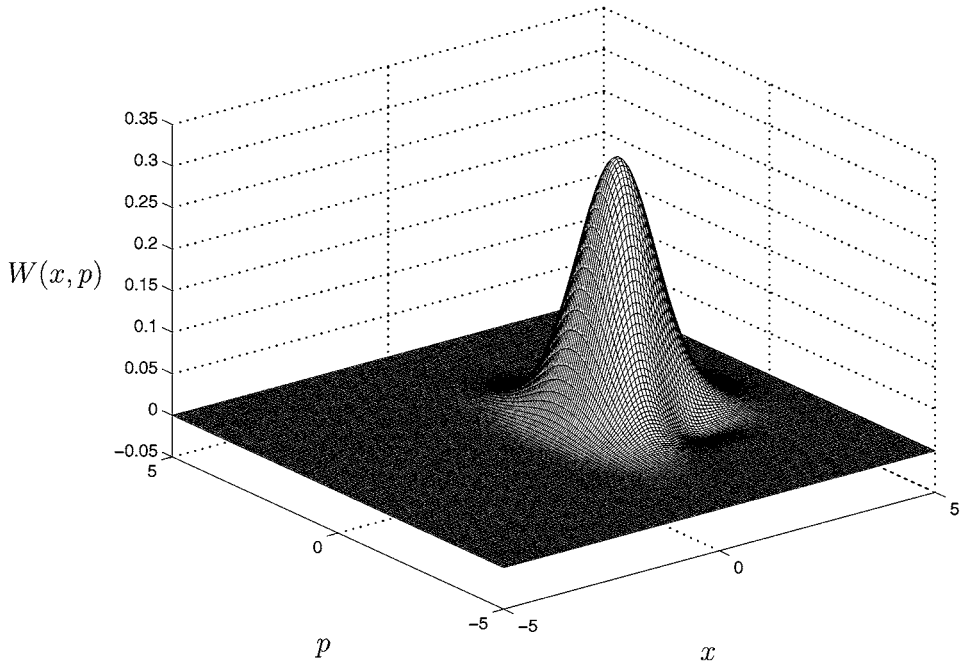

Figure 6. The Wigner function of the GK coherent state $|J = 2, \theta = 0; \omega = 1, \lambda = 1, \mu = 1\rangle$. The truncation $N_{\max} = 15$.

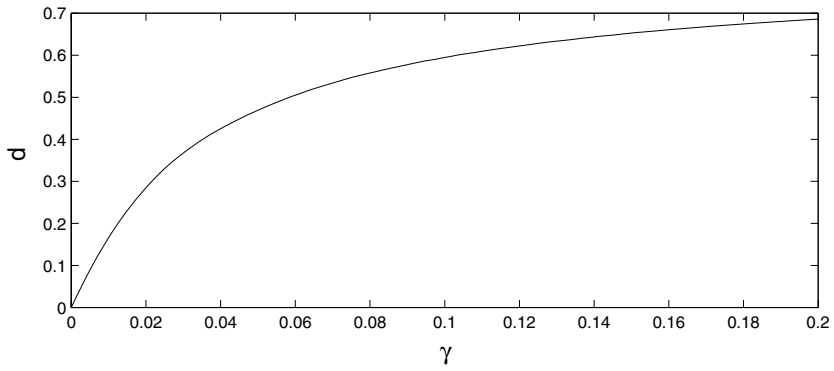

Figure 7. For each value of γ, the system is evolved from $t = 0$ to $t = 6.3/\omega$. The distance (17) with $p = 2$ between this evolved state and the evolved state for $\gamma = 0$ is then calculated and plotted. The damped model (20) with $\omega = 1$, $\lambda = 1$, $\mu = 1$, $N_{\max} = 15$ and $M = 1$ is used. The initial state is the GK coherent state $|J = 2, \theta = 0; \omega, \lambda, \mu\rangle$.

Taking the matrix elements of the operators of equation (20) with respect to number eigenstates, we get

$$\frac{\partial \rho_{mn}}{\partial t} = \mathrm{i} \sum_k [H_{mk}\rho_{kn} - \rho_{mk}H_{kn}] + \frac{\gamma}{2}(M+1)\left[2\sqrt{(m+1)(n+1)}\,\rho_{m+1,n+1} - (m+n)\rho_{mn}\right] + \frac{\gamma}{2}M\left[2\sqrt{mn}\,\rho_{m-1,n-1} - (m+n+2)\rho_{mn}\right]. \tag{22}$$

We solved numerically this equation using truncated matrices as discussed in the appendix.

In figure 3 (solid curves) we present quantum statistics for the damped model when the system is initially in a GK coherent state. It is seen that $\langle N\rangle$ decreases as the system loses quanta to the environment, and that even though the initial state is a GK coherent state for the system, $g^{(2)}$ increases, and approaches 2 around $\omega t = 20$, so the coherence is lost by this time, and the system is in a thermal state.

In figure 7 we present the distance (17) as a function of the damping rate γ of equation (20). For each value of γ, the system is evolved from the initial GK coherent state $|J = 2, \theta = 0; \omega, \lambda, \mu\rangle$ to time $t = 6.3/\omega$. The distance between this evolved state and the evolved state for $\gamma = 0$ is then calculated. It is seen that increasing the damping rate destroys the coherence rapidly.

5. Time evolution of the ordinary coherent states in this system

Above, we have studied the GK coherent states for the Hamiltonian (1), which are specially constructed so that evolution of such a state is another state of this kind (temporal stability property). We stress that the ordinary coherent states [7] do not have this property for the Hamiltonian (1). In order to see this explicitly we calculate in this section how the ordinary coherent states evolve in time. We have considered the case where the initial state is an ordinary coherent state $|A\rangle$ with $A = 2$.

In figure 8 (broken curves in the absence of dissipation) we plot the average number of photons $\langle N\rangle$ and the second-order correlation $g^{(2)}$ functions of time. It is seen that the average number of photons $\langle N\rangle$ varies with time, and that $g^{(2)} < 1$ for $\omega t > 0$, so the initial coherent state becomes squeezed and remains so. We also present results for the damped model (solid curves). It is seen that $\langle N\rangle$ decreases with time and that $g^{(2)}$ increases with time,

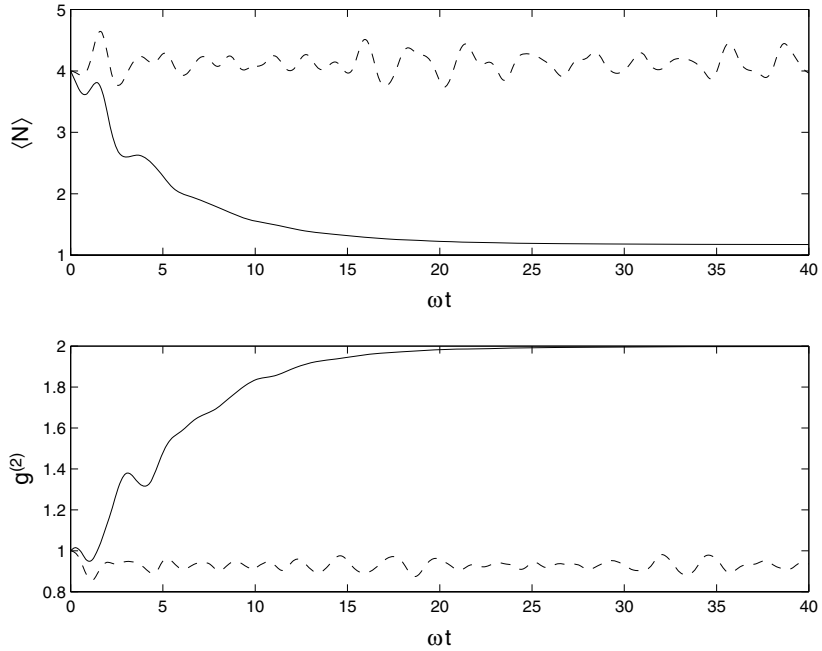

Figure 8. The upper graph shows the average number of photons $\langle N\rangle$ with $\omega = 1$, $\lambda = 1$, $\mu = 1$, $M = 1$, $N_{\max} = 15$ and initial state $|A = 2\rangle$. The solid curve shows damped results ($\gamma = 0.2$), and the broken curve shows undamped results ($\gamma = 0$). The lower graph shows the second-order correlation $g^{(2)}$ for the same system (solid curve shows $\gamma = 0.2$, broken curve shows $\gamma = 0$).

and reaches the value 2 around $\omega t = 20$. This shows that by this time the coherence of the initial state has been lost, and the system is now in a thermal state.

The decoherence time is defined as follows. From figure 8, we see that in the presence of dissipation, $g^{(2)}$ may be approximated by

$$g^{(2)}(t) \approx 2 - A\exp(-t/\tau) \tag{23}$$

for some constants A and τ. We call τ the decoherence time. Using the numerical results of figure 8, we obtain $\tau \approx 6.3/\omega$.

6. Generation of Schrödinger cats

Since the evolution operator contains the exponential of the displacement operator $D(\mathrm{i}\mu)$, which can be written as a sum of terms of the form $D(\mathrm{i}\mu)$, $D(2\mathrm{i}\mu)$, $D(3\mathrm{i}\mu)$, ..., we expect that the initial state $|s(0)\rangle$ will evolve into a superposition of 'displaced states' $D(\mathrm{i}\mu)|s(0)\rangle$, $D(2\mathrm{i}\mu)|s(0)\rangle$, $D(3\mathrm{i}\mu)|s(0)\rangle$, ... ('generalized Schrödinger cats'). In order to demonstrate this we have calculated the probability distribution of the state $|s(t)\rangle = \sum s_N(t)|N\rangle$

$$|s(x,t)|^2 = \left|\sum s_N(t)\langle x|N\rangle\right|^2. \tag{24}$$

Assuming that the system is initially in an ordinary coherent state, we present in figures 9 and 10 the probability distribution (24) for the cases of no dissipation and dissipation with $\gamma = 0.01$ and $M = 1$, correspondingly. As expected, it is seen that the initial coherent state evolves into a superposition or mixture of displaced states. In the case of no dissipation we

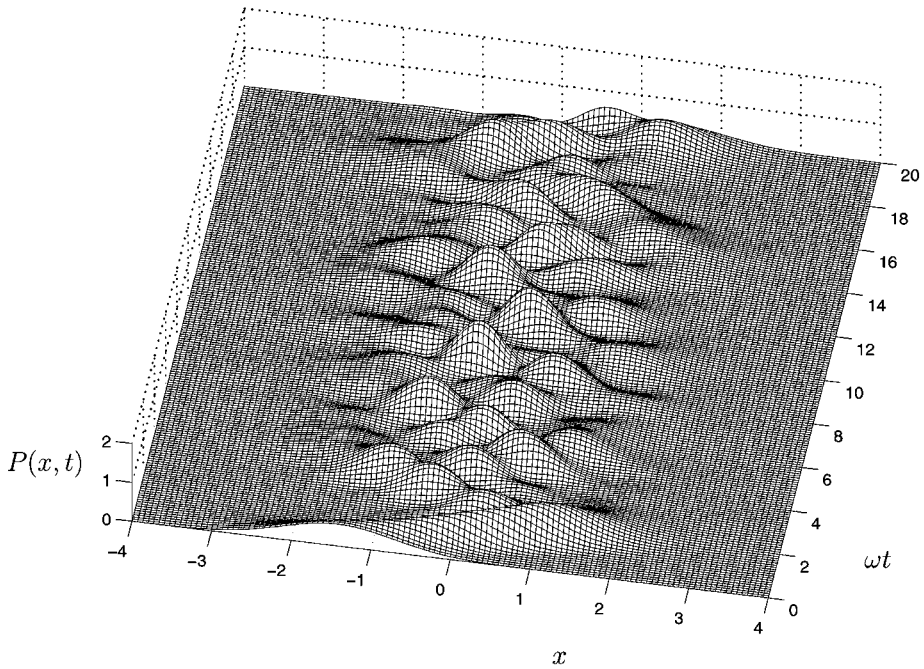

Figure 9. The evolution of a coherent state under the Hamiltonian (1) with $\omega = 1, \lambda = 2, \mu = 1$ and $N_{\max} = 15$. The initial state is $|A = -1\rangle$. The probability distribution of equation (24) is plotted. The system evolves into a superposition of macroscopically distinguishable states—'generalized Schrödinger cats'.

know that the system is always in a pure state and therefore we are confident that we have a superposition of displaced states. In the dissipative case the system evolves into a mixed state and for this reason we study in more detail these states with the Wigner function.

In figures 11 and 12 we present the Wigner function for the system at time $t = 15.3$ for the dissipationless and dissipative case correspondingly. It is seen that the effect of the dissipation is to destroy the inteference parts.

7. Discussion

We have considered a Hamiltonian with sinusoidal nonlinearity (1) and introduced Gazeau–Klauder coherent states for this Hamiltonian. We have studied the uncertainty properties and the quantum statistical properties of these states and shown that as λ increases, they deviate considerably from those of the ordinary coherent states. We have calculated how fast the dissipation destroys the Gazeau–Klauder coherent states for our model.

We have also considered ordinary coherent states and shown that in the absence of dissipation, they evolve into superpositions of many macroscopically distinguishable states ('multi-Schrödinger cats'). The effect of dissipation on these states has been quantified.

From a practical point of view, extensions of the Hamiltonian that we have considered can be used for the description of mesoscopic Josephson devices (e.g. [5]) which are currently one of the candidates for quantum gates. From a theoretical point of view, the periodic nature of the potential makes the model very interesting. For example, the displacement operator appears in the Hamiltonian, and consequently the exponential of the displacement operator

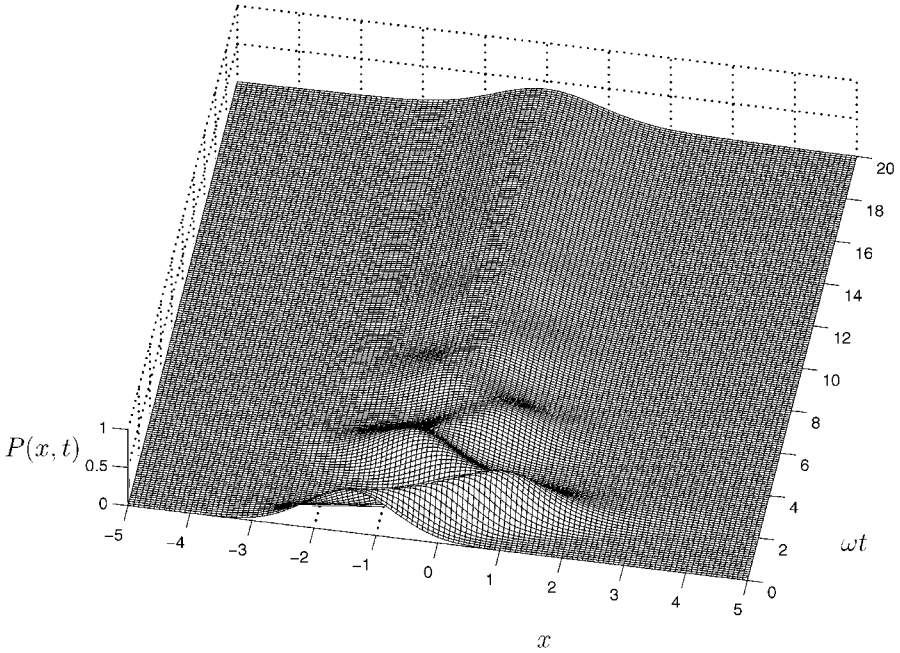

Figure 10. The evolution of a coherent state under the damped model (20) with $\omega = 1$, $\lambda = 2$, $\mu = 1$, $N_{\max} = 15$ and damping parameters $\gamma = 0.2$, $M = 1$. The initial state is $|A = -1\rangle$. The probability distribution of equation (24) is plotted. It is seen that the superpositions of macroscopically distinguishable states no longer occur because of the dissipation.

appears in the evolution operator. The properties of the latter have not been studied before. In this paper, we have used the exponential of the displacement operator in our numerical work, and therefore we got a feeling about its properties, but there is no doubt that this is a subject in its own right, which deserves further work.

Appendix

We solve the truncated equation (22) by converting it into the form

$$\frac{\mathrm{d}r}{\mathrm{d}t} = \mathcal{A}r \tag{25}$$

where r is a 'density vector', and, $\mathcal{A}$ is an 'appropriate' matrix.

By 'density vector' we mean a vector representation of the truncated density matrix ρ_{mn}. Since ρ_{mn} is $N_{\max} + 1$ by $N_{\max} + 1$, r will be $(N_{\max} + 1)^2$ by 1. The entries of r are given by stacking the columns of ρ_{mn} on top of each other:

$$r^T = (\rho_{00}, \rho_{10}, \ldots, \rho_{N_{\max},0}, \rho_{01}, \ldots, \rho_{N_{\max},1}, \ldots, \rho_{0,N_{\max}}, \ldots, \rho_{N_{\max},N_{\max}}). \tag{26}$$

The matrix $\mathcal{A}$, is such that its action on the density vector r is the same as the action of the combination of the operators H, a, $a^\dagger$, on the density matrix ρ in equation (20). Since r is $(N_{\max} + 1)^2$ by 1, $\mathcal{A}$ will be $(N_{\max} + 1)^2$ by $(N_{\max} + 1)^2$. In general, if B acts on the left of ρ, the corresponding appropriate matrix $\mathcal{B}$ is obtained by putting $N_{\max} + 1$ copies of B along

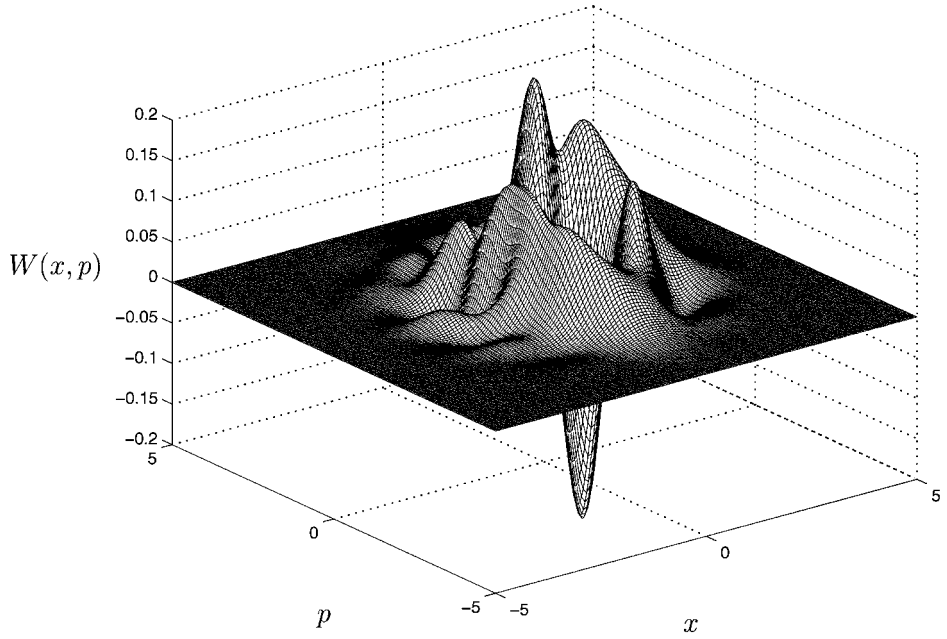

Figure 11. The Wigner function for the state of the system at time $t = 15.3$ using the undamped model. The system is evolved from the initial state $|A = -1\rangle$, and $\omega = 1$, $\lambda = 2$, $\mu = 1$, $N_{\max} = 15$.

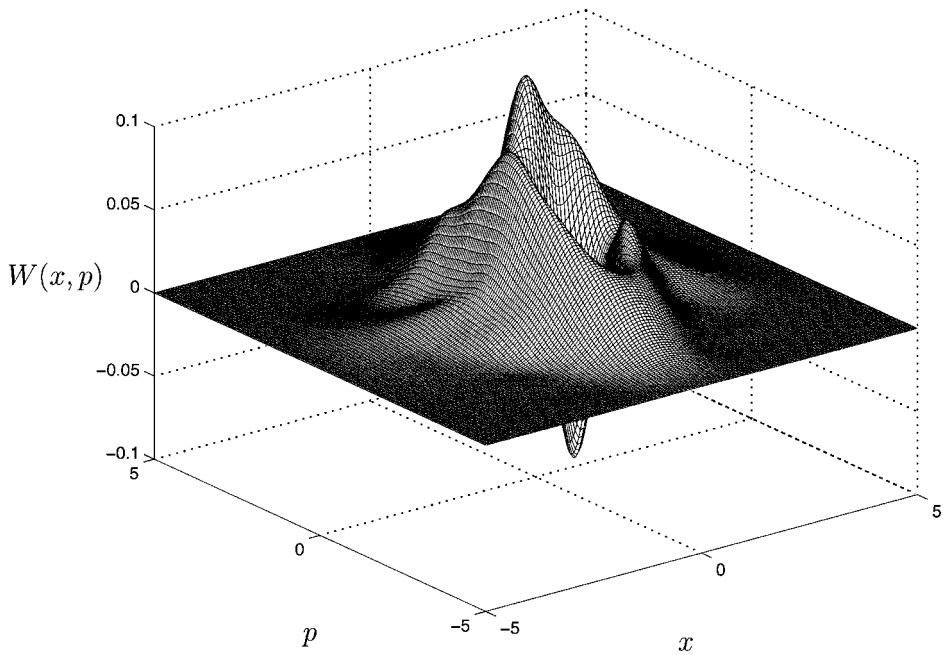

Figure 12. The Wigner function for the state of the system at time $t = 15.3$ using the damped model. The system is evolved from the initial state $|A = -1\rangle$, and $\omega = 1, \lambda = 2, \mu = 1, \gamma = 0.01$, $M = 1$, $N_{\max} = 15$. It is seen that the effect of the dissipation is to destroy the inteference parts.

the leading diagonal:

$$\mathcal{B}_{kl} = \begin{cases} B_{mn} & \text{if} \quad k = p(N_{\max}+1)+m \quad l = p(N_{\max}+1)+n \\ & \text{where} \quad 0 \leqslant p, m, n \leqslant N_{\max} \\ 0 & \text{otherwise.} \end{cases} \tag{27}$$

For example, the matrix equation

$$H\rho = \begin{pmatrix} a & c \\ b & d \end{pmatrix} \begin{pmatrix} w & y \\ x & z \end{pmatrix} = \begin{pmatrix} aw+cx & ay+cz \\ bw+dx & by+dz \end{pmatrix} \tag{28}$$

becomes the vector equation

$$\mathcal{H}r = \begin{pmatrix} a & c & & \\ b & d & & \\ & & a & c \\ & & b & d \end{pmatrix} \begin{pmatrix} w \\ x \\ y \\ z \end{pmatrix} = \begin{pmatrix} aw+cx \\ bw+dx \\ ay+cz \\ by+dz \end{pmatrix}. \tag{29}$$

If C acts on the right of ρ, the corresponding appropriate matrix $\mathcal{C}$ is given by interlacing inflated copies of the *transpose* of C (not $C^{\dagger}$) along the leading diagonal:

$$\mathcal{C}_{kl} = \begin{cases} C_{nm} & \text{if} \quad k = p+m(N_{\max}+1) \quad l = p+n(N_{\max}+1) \\ & \text{where} \quad 0 \leqslant p, m, n \leqslant N_{\max} \\ 0 & \text{otherwise.} \end{cases} \tag{30}$$

For example, the matrix equation

$$\rho H = \begin{pmatrix} w & y \\ x & z \end{pmatrix} \begin{pmatrix} a & c \\ b & d \end{pmatrix} = \begin{pmatrix} aw+by & cw+dy \\ ax+bz & cx+dz \end{pmatrix} \tag{31}$$

becomes

$$\mathcal{H}r = \begin{pmatrix} a & & b & \\ & a & & b \\ c & & d & \\ & c & & d \end{pmatrix} \begin{pmatrix} w \\ x \\ y \\ z \end{pmatrix} = \begin{pmatrix} aw+by \\ ax+bz \\ cw+dy \\ cx+dz \end{pmatrix}. \tag{32}$$

Acknowledgments

We are grateful to Professor J-P Gazeau for helpful discussions. JMH and AK gratefully acknowledge support from EPSRC.

References

[1] Nieto M M and Simmons L M 1978 *Phys. Rev. Lett.* **41** 207
Nieto M M 1980 *Phys. Rev.* D **22** 391
Nieto M M 1984 *Phys. Rev.* D **30** 770
[2] Perelomov A M 1986 *Generalized Coherent States and Their Applications* (Berlin: Springer)
Klauder J R and Skagerstam B-S 1985 *Coherent States* (Singapore: World Scientific)
[3] Klauder J R 1995 *Ann. Phys., NY* **237** 147
Klauder J R 1996 *J. Phys. A: Math. Gen.* **29** L293
[4] Gazeau J-P and Klauder J R 1999 *J. Phys. A: Math. Gen.* **32** 123
[5] Vourdas A and Spiller T P 1997 *Z. Phys.* B **102** 43
[6] Feynman R P 1951 *Phys. Rev.* **84** 108
Schwinger J 1953 *Phys. Rev.* **91** 728
Roy S M and Singh V 1982 *Phys. Rev.* D **25** 3413
Venkata Satyanarayana M 1985 *Phys. Rev.* D **32** 400
[7] Glauber R J 1963 *Phys. Rev.* **130** 2529